Journal of Tissue Engineering
Volume 9: 1–9

DOI: 10.1177/2041731418764709
journals.sagepub.com/home/tej

Toward a patient-specific tissue engineered vascular graft

Cameron Best[1,2], Robert Strouse[3], Kan Hor[4], Victoria Pepper[1,5], Amy Tipton[6], John Kelly[1,4], Toshiharu Shinoka[1,7] and Christopher Breuer[1,5]

Abstract

Integrating three-dimensional printing with the creation of tissue-engineered vascular grafts could provide a readily available, patient-specific, autologous tissue source that could significantly improve outcomes in newborns with congenital heart disease. Here, we present the recent case of a candidate for our tissue-engineered vascular graft clinical trial deemed ineligible due to complex anatomical requirements and consider the application of three-dimensional printing technologies for a patient-specific graft. We 3D-printed a closed-disposable seeding device and validated that it performed equivalently to the traditional open seeding technique using ovine bone marrow–derived mononuclear cells. Next, our candidate's preoperative imaging was reviewed to propose a patient-specific graft. A seeding apparatus was then designed to accommodate the custom graft and 3D-printed on a commodity fused deposition modeler. This exploratory feasibility study represents an important proof of concept advancing progress toward a rationally designed patient-specific tissue-engineered vascular graft for clinical application.

Keywords

Tissue-engineered vascular graft, 3D-printing, Fontan operation, patient-specific modeling, cell seeding

Date received: 27 November 2017; accepted: 20 February 2018

Background

Congenital cardiac anomalies are the leading cause of death in the newborn period and approximately 25% of these patients require cardiac surgery in the first years of life.[1–3] Patients with univentricular heart disease bear a large burden of the morbidity and mortality associated with congenital heart disease and present unique and challenging management decisions. These patients typically undergo staged palliation procedures to ultimately connect the systemic venous return passively to the pulmonary arteries and utilize a single ventricle for systemic cardiac output. The Fontan operation is the final palliative step at which time the inferior vena cava is directly connected to the pulmonary arteries. Lack of suitable autologous tissue for construction of a large caliber blood vessel necessitates the use of synthetic materials for the Fontan conduit, and the current standard of care is to use Dacron® or GoreTex® grafts. While use of synthetic materials for vascular grafting carries a known risk of infection, rejection,

[1]Center for Regenerative Medicine, The Research Institute, Nationwide Children's Hospital, Columbus, OH, USA
[2]Biomedical Sciences Graduate Program, The Ohio State University College of Medicine, Columbus, OH, USA
[3]Research Innovation and Solutions, The Research Institute, Nationwide Children's Hospital, Columbus, OH, USA
[4]Department of Cardiology, The Heart Center, Nationwide Children's Hospital, Columbus, OH, USA
[5]Department of Surgery, Nationwide Children's Hospital, Columbus, OH, USA
[6]Advanced Cardiac Imaging Laboratory, The Heart Center, Nationwide Children's Hospital, Columbus, OH, USA
[7]Department of Cardiothoracic Surgery, The Heart Center, Nationwide Children's Hospital, Columbus, OH, USA

Corresponding author:
Cameron Best, Center for Regenerative Medicine, The Research Institute, Nationwide Children's Hospital, 575 Children's Crossroad—WB4154, Columbus, OH 43215, USA.
Email: Cameron.Best@nationwidechildrens.org

calcification, aneurysm, thrombosis, and/or stenosis, the Fontan physiology is particularly sensitive to graft geometry in that a suboptimal hemodynamic profile can limit pulmonary blood flow and result in systemic venous congestion with deleterious consequences, including the development of chronic liver disease and protein losing enteropathy.[4] Consequently, a common approach is to oversize the Fontan conduit, thereby allowing a child to "grow into" their graft; however, this technique can lead to non-laminar flow, mural thrombus, and intimal hyperplasia, which can progress to critical stenosis.[5–9] The long-term performance of traditionally utilized synthetic grafts is understudied, yet recent research has demonstrated that poor biocompatibility, lack of growth potential, and suboptimal graft geometry contributes to the incidence of reoperation and/or endovascular intervention.[10,11]

Our group has pursued the development of a tissue-engineered vascular graft (TEVG) for use in the Fontan operation.[12–14] A completely autologous Fontan graft would be a significant improvement to the current standard of care if optimized to mitigate the complications associated with synthetic materials and provide the added benefit of size matching and growth potential. We are currently amidst the first Food and Drug Administration (FDA)-approved clinical trial (FDA IDE 14127) evaluating the use of bone marrow mononuclear cell (BM-MNC) seeded TEVGs in the pediatric population and four patients have received TEVGs in the United States to date. The most significant benefit of the TEVG is its biodegradability, which renders a completely autologous vascular conduit that can grow and remodel with its host, obviating the risk of serial reoperation to upsize the graft due to somatic overgrowth.[15,16] Currently used scaffolds in our clinical trial comprise a knitted polyglycolic acid (PGA) tube sealed with a 50:50 copolymer solution of L-lactide-ε-caprolactone (PLCL) and are provided by Gunze, Ltd. (Kyoto, Japan).[12] The biocompatibility and *in vivo* degradation profiles of PGA and PLCL have been extensively studied; these polyesters degrade via ester hydrolysis into naturally occurring metabolites, and both are FDA approved.[17,18] While promising, our approach is limited by many of the same challenges facing synthetic graft materials, primarily (1) the TEVG is not resistant to stenosis and (2) only linear scaffolds of constant diameter are currently available (13 cm long with inner diameters ranging from 10 to 20 mm in increments of 1 mm). Ultimately, cases of complex anatomy that could not be sufficiently addressed with an isodiametric linear graft can render a Fontan candidate ineligible to receive a TEVG in our trial. A further limitation is that the time, labor, and resource-intensive nature of TEVG preparation along with the complexities of maintaining a Good Manufacturing Practice (GMP)-compliant clean room limit the widespread adoption of the BM-MNC seeded TEVG.

Approach

In the past decade, patient-specific Fontan graft geometries have been proposed born from strides in the computational modeling of univentricular hemodynamics. Integration between clinicians and engineers has provided patient-specific models to predict Fontan outcomes and direct clinical decision-making.[19,20] This multidisciplinary approach has provided a critical first step in the surgical planning,[21] computational simulation,[22] and optimization[23] of Fontan conduits in the congenital heart population. Furthermore, advances in additive manufacturing promise the ability to generate patient-specific regenerative implants for cardiovascular applications.[24–26] Incorporating patient-specific modeling and customized regenerative implants to yield an optimized patient-specific TEVG is a natural extension of significant progress in both fields. However, the feasibility of this integration into a seamless, safe, and efficacious clinical protocol is currently theoretical and the subject of ongoing investigation.

We recently established the feasibility of implanting nonlinear cell-free TEVGs in a juvenile lamb model with relative success.[27] In this study, a TEVG scaffold was co-electrospun from PGA and PLCL onto a custom 3D-printed mandrel. Grafts were implanted in an ovine model for 6 months and evaluated for patency and neotissue formation. No adverse events were encountered and the custom electrospun TEVG performed comparably to traditional linear scaffolds in the same large animal model.[15] While promising, this study examined too few animals over too short a time course to advocate adoption of cell-free electrospun grafts. In fact, in a murine model, the co-electrospun PGA/PLCL scaffold required autologous cell seeding to maintain graft patency.[28] This result is consistent with both murine and ovine work from our group reporting that BM-MNC seeding reduces the acute host inflammatory responses that contribute to the development of intimal hyperplasia and the progression of stenosis.[29–32] In fact, we recently described a dose-responsive effect of BM-MNC seeding, which indicated that an approximately fourfold increase in the number of seeded cells could effectively prevent the development of TEVG stenosis.[30] Thus, we propose that the second-generation TEVG should be optimized to the anatomical and physiological requirements of each recipient and seeded with a high dose of BM-MNCs.

The current clinical protocol for manufacture of the TEVG is an intricate and coordinated effort between a multidisciplinary team (Figure 1). Briefly, on the day of implantation, 5 mL/kg of bone marrow is aspirated from the iliac crests of the graft recipient. Bone marrow is delivered to an ISO Class 7 Clean room where mononuclear cells are enriched via density gradient centrifugation and two sequential washes of phosphate-buffered saline (PBS). During BM-MNC enrichment, the surgeon begins the Fontan operation and determines the appropriate graft size, which is

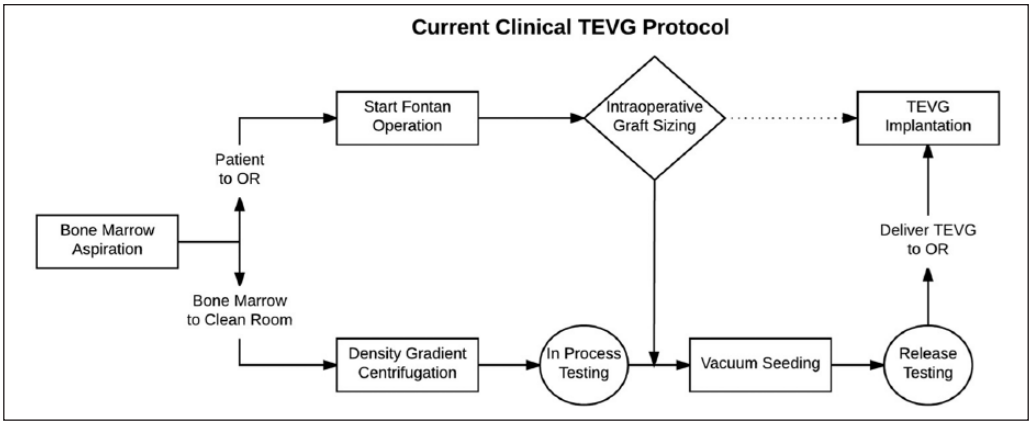

Figure 1. Flowchart of the current clinical TEVG fabrication protocol. Boxed items indicate process components, diamonds highlight a critical process decision, and circles indicate release testing. Briefly, 5 mL/kg whole bone marrow is aspirated from the iliac crests of the Fontan patient prior to operation. After aspiration, the patient is prepped for Fontan completion and dissection is begun. The bone marrow is delivered to an ISO Class 7 Clean room where mononuclear cells are enriched via density gradient centrifugation. Samples for in-process testing are collected and include cell viability and CD45 flow cytometry. The seeding team waits for a call from the operating room, which communicates the appropriate graft diameter based on intraoperative conduit sizing. The graft is selected and seeded via an operator independent vacuum method. Samples are collected for release testing and include Gram staining of a graft sample, dsDNA assay, and seeding efficiency. Sterility cultures are also collected for post-process monitoring. If all tests pass the criteria, then the seeded TEVG scaffold is delivered to the operating room for implantation.

communicated to the clean room team. Per the intraoperative sizing, a scaffold is selected and affixed to a fenestrated mandrel. The mandrel and scaffold are then placed in a graduated cylinder and PBS is added to submerge the scaffold. Negative pressure is applied (−5 to −10 mmHg) and the scaffold is "pre-wet" with the PBS. Next, the enriched BM-MNCs are added and vacuumed through the scaffold's wall, embedding BM-MNCs within its pores. The seeded graft is removed from the mandrel and sampled to evaluate seeding efficiency and sterility (among other criteria) prior to release to the operating room for implantation.

More recently, we have replaced this labor-intensive, complex process with a closed disposable filtration/elution system. We have previously characterized and determined the biological equivalency of a closed disposable filtration/elution system for BM-MNC enrichment.[33–35] Not only does this method accomplish BM-MNC enrichment in less than 1 h, use of multiple filters in parallel would permit the processing of greater bone marrow volumes which could be used to increase the seeded cell dose by providing a greater number of BM-MNCs in the preseeding solution. What has been unexplored to date, however, is the seeding of a scaffold with nonlinear geometry and nonconstant diameter. Additive manufacturing has recently become the gold standard for rapid fabrication of custom implant grade medical devices,[24,36–38] and we sought to examine its potential within the context of TEVG seeding. We utilized computer-aided drafting (CAD) to recapitulate a previously proposed closed seeding apparatus that attaches to the Luer Lock of the filtration/elution system (Figure 2).[33] This apparatus was then 3D-printed from polylactic acid (PLA) filament using a fused deposition modeler (Ultimaker 2) and sterilized with ethylene oxide gas. We used the previously described closed filtration/elution system (HemaTrate™ System, Cook Regentec, Indianapolis, IN) to enrich BM-MNCs from an aspirate of juvenile lamb bone marrow (60 mL whole bone marrow).[34,35] A current clinical scaffold (14 mm inner diameter) was then vacuum seeded with the eluted BM-MNCs using our 3D-printed apparatus. As previously described, seeding is accomplished without the use of bioreactor culture and relies upon the applied vacuum pressure and porosity of the scaffold to embed cells within its walls.[32–34,39] The seeded scaffold was sampled for determination of seeding efficiency (hematology analysis of pre- and postseeding solutions) and cell density (PicoGreen dsDNA assay) and passed current release criteria ($25{,}983 \pm 6195$ cells/mm^3 > 1000 cells/mm^3, and 40.48% > 10% seeding efficiency). BM-MNC cell nuclei were identified within the pores of a frozen section of a mid-graft sample, confirming DNA assay findings (Figure 2). The 3D-printed seeding apparatus performed equivalently to that of the traditional open seeding setup. Encouraged by these preliminary data, we sought to apply the novel approach to a relevant clinical scenario in which a currently available scaffold and the traditional seeding technique would be inadequate.

Application

A 10-year-old male was diagnosed with heterotaxy syndrome with asplenia, dextrocardia, right dominant atrioventricular canal defect with a severely hypoplastic left ventricle, double outlet right ventricle with malposed great

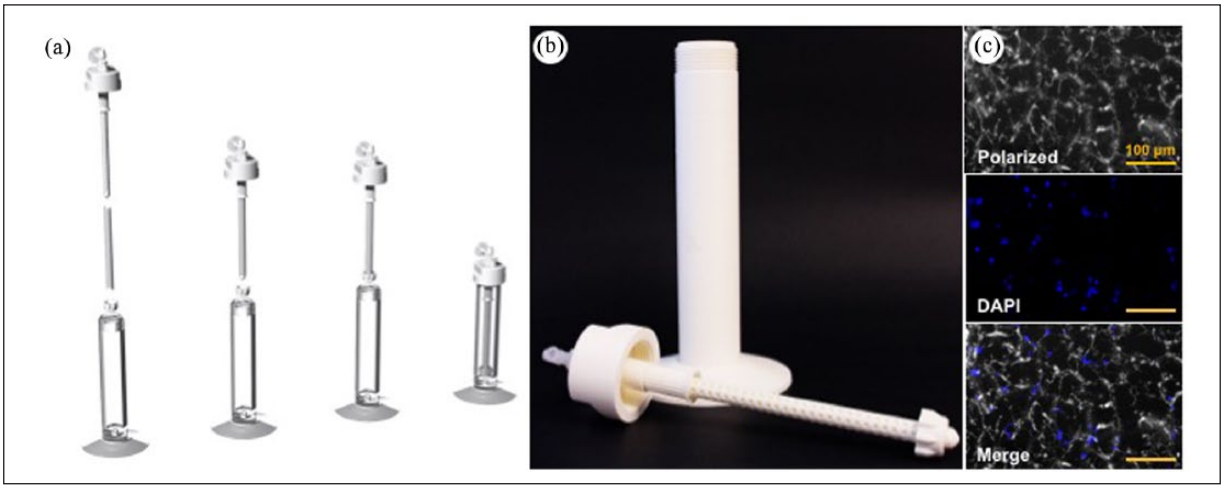

Figure 2. (a) Rendering of 3D-printed closed, disposable seeding system for preparation of currently utilized TEVG scaffolds. (b) Photographs of 3D-printed prototype utilized in this report. (c) 20× photomicrograph of seeded scaffold section stained with DAPI visualized with polarized transmitted (top) and fluorescent reflected light (middle) to identify birefringent scaffold polymer and seeded cell nuclei, respectively. The merged image (bottom) reveals seeded BM-MNCs embedded within the porous scaffold wall and confirms dsDNA assay results.

arteries with subpulmonary stenosis, and supracardiac total anomalous pulmonary venous return (TAPVR) to the superior vena cava. The patient had undergone TAPVR repair and received a bidirectional Glenn shunt in preparation for the Fontan completion. Cardiac magnetic resonance imaging (CMR) was obtained and his case proposed by the cardiology team at Nationwide Children's Hospital (Columbus, OH) for enrollment in the clinical trial to receive a Fontan TEVG (Figure 3). Unfortunately, the patient was deemed ineligible for enrollment due to overly complex anatomy and the need for a nonlinear TEVG conduit. This case represents a situation in which the ideal Fontan conduit would not be the currently utilized scaffold, and offered a unique opportunity to explore the feasibility of a patient-specific TEVG and 3D-printed seeding apparatus.

CAD and the reconstructed CMR imaging were used to design a custom TEVG scaffold. Notable features of the first patient-specific TEVG were its nonconstant diameter (ranging from 18 to 24 mm), overall length greater than 13 cm (14.5 cm), and the presence of a doubly meandering compound curve. We first designed the seeding mandrel to accommodate the theoretical graft using a double-helixed lattice terminating with the cap of the seeding chamber. There was remarkable similarity between the custom designed scaffold and mandrel and the shape adopted by the traditional Gore-Tex conduit used in this patient for his Fontan completion (Figure 4). The seeding chamber was designed to hold the volume of scaffold, mandrel, and 120 mL of enriched BM-MNCs from our filtration/elution system, which would correspond to a 20 mL/kg aspiration from a 10-kg child (a fourfold higher dose than our current clinical protocol). The inlet and outlet (preseeding and postseeding solutions, respectively) are connected to the either the filtration/elution system's transfusion tubing (inlet) or vacuum tubing from the specimen traps (outlet) via Luer Lock and barbed ports. A final air inlet was fitted with a 40-µm sterile air filter (Figure 5). The assembly of the graft, mandrel, and seeding chamber would be performed in a sterile field during the operation at the bedside and sterile connections made to the closed disposable filtration/elution system. The CMR reconstruction/analysis, design of the custom graft and seeding apparatus, and 3D-printing the seeding device required a total of 36 h.

Future directions

The design criteria for the graft discussed in this report were purely anatomic in nature, but future iterations of this approach would incorporate fluid dynamic computational modeling, among other predictive in silico techniques to model the optimal graft geometry on macro, micro, and nanoscales.[19,21,22,25,40] A well-powered large animal study evaluating the long-term performance of custom BM-MNC seeded TEVGs would be required before advocating translation to the clinic. A challenge to overcome will be the difficulty in recapitulating the complex anatomies required in the pediatric congenital heart population in the native juvenile lamb model. In addition, it will be critically important to redefine the current clinical protocol to include preoperative TEVG planning, scaffold design, seeding apparatus manufacturing, and BM-MNC enrichment/scaffold seeding. The proposed pipeline to rapidly fabricate and seed an optimized patient-specific TEVG (Figure 6) begins with the preoperative imaging studies. Reconstructed CMR images would be used to determine the anatomical requirements of the patient receiving the Fontan conduit, then fluid

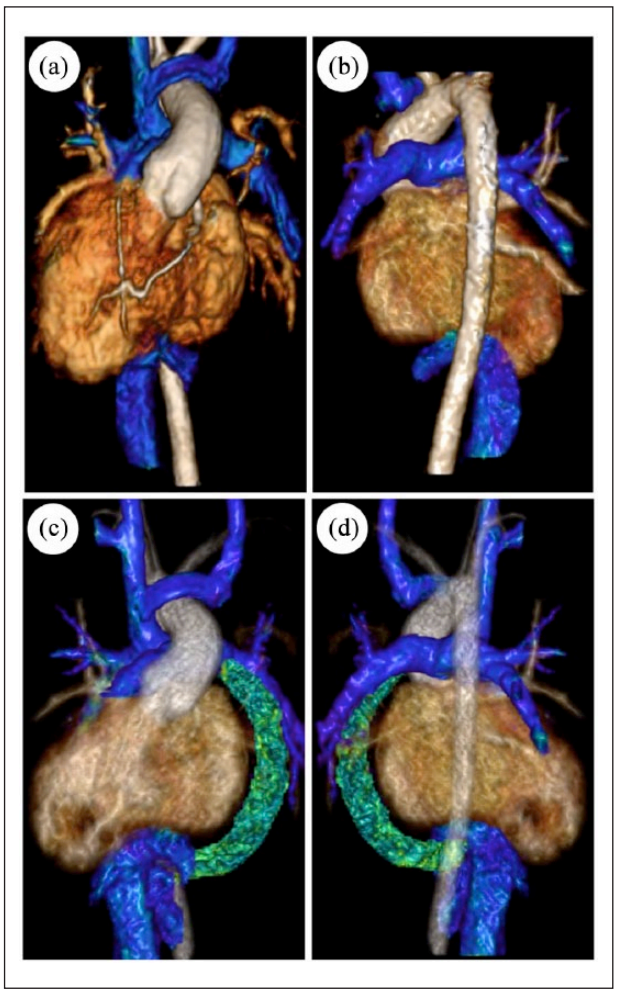

Figure 3. Preoperative CMR reconstructions of a candidate Fontan TEVG patient in the (a) coronal plane viewed from the (a) anterior-posterior and (b) posterior–anterior perspectives. The patient presented with heterotaxy syndrome, asplenia, associated dextrocardia, right dominant atrioventricular canal defect with a severely hypoplastic left ventricle, double outlet right ventricle with malposed great arteries with subpulmonary stenosis, and total anomalous pulmonary venous return (TAPVR) to the superior vena cava status post TAPVR repair and bidirectional Glenn shunting. CAD was used to propose a patient-specific TEVG conduit, which was superimposed on the CMR reconstructions. The proposed Fontan conduit is highlighted in green and viewed in the coronal plane from the (c) anterior–posterior and (d) posterior–anterior perspectives.

dynamic and mechanobiologic computational modeling employed to determine the optimal scaffold design in silico. The scaffold would then be electrospun on a 3D-printed mandrel corresponding to the patient-specific design as previously described.[27] In parallel, the custom seeding mandrel and chamber would be designed and 3D-printed as described in this report. Scaffold and seeding apparatus would be sterilized via ethylene oxide gas or γ-irradiation, delivered to the surgical team during bone marrow aspiration, and connected to the closed disposable filtration/elution system in a sterile fashion. BM-MNCs would be enriched via the closed filter, eluted to the seeding chamber containing mandrel and scaffold, and a vacuum applied to complete seeding as previously described. This workflow, although speculative, would allow for a readily available patient-specific TEVG for point-of-care treatment of congenital heart disease and is the focus of our ongoing translational efforts.

Methods

Animal care and ethics statement

The Institutional Animal Care and Use Committee of the Research Institute at Nationwide Children's Hospital (Columbus, OH) reviewed and approved the protocol (AR13-00079). Representatives of the Animal Care staff monitored the animal utilized in this study both intraoperatively and during recovery. The experimental procedure and animal care was within the humane guidelines published by the Public Health Service, National Institutes of Health (Bethesda, MD) in the Care and Use of Laboratory Animals (2011), as well as USDA regulations set forth in the Animal Welfare Act.

Bone marrow harvest

One juvenile sheep (*Ovis aries*, 25 kg) underwent bone marrow harvest for scaffold seeding. The sheep was induced using a cocktail of ketamine (10 mg/kg) and diazepam (0.5 mg/kg) and the anesthetic plane was maintained with isoflurane (1%–4% in 100% O_2). The animal was placed in lateral recumbent position and the area overlying the iliac crest was prepped and draped in standard sterile fashion. A 2-mm incision was made over the bony prominence and the iliac crest was cannulated with an Illinois aspiration needle (15G, CareFusion; Vernon Hills, IL). Heparinized syringes (100 U/mL in normal saline) were used to aspirate 60 mL of bone marrow, which was transported to a biosafety cabinet for mononuclear cell enrichment and scaffold seeding using the 3D-printed closed-disposable system as previously described.[33–35,39]

DNA assay

Immediately following graft seeding, the scaffold (13 cm × 1.4 cm) was sectioned into 5 × 5 mm^2 samples from the top, middle, or bottom ($n = 5$ sections/region) for determination of seeded cell density. An aliquot of the pre-seeding BM-MNC solution was used to generate a standard curve of known cell concentration via serial dilution. The samples and standards were incubated in dH_2O at −80°C in a 96-well plate to induce cell lysis. The double-stranded DNA concentration of a 50 µL aliquot of each sample was determined via fluorometric Quant-iT™ PicoGreen™ dsDNA assay, following the manufacturer's protocol (ThermoFisher Scientific).

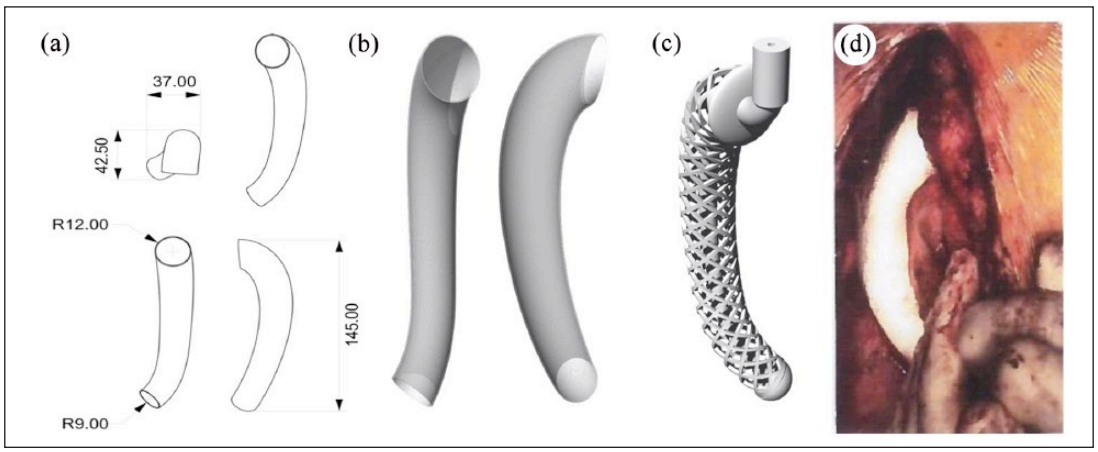

Figure 4. (a) Design of patient-specific TEVG conduit demonstrating a compound curve and lumen diameter changing 3.0 mm from the proximal to distal anastomoses. (b) 3D renderings of (a). (c) A custom fenestrated seeding mandrel was reverse-engineered from the proposed scaffold. (d) Intraoperative photograph from the proposed TEVG candidate after implantation of a standard-of-care Gore-Tex conduit. Note that the linear conduit adopted a nonlinear shape in response to patient anatomy, which closely resembles the geometry of the proposed patient-specific TEVG scaffold.

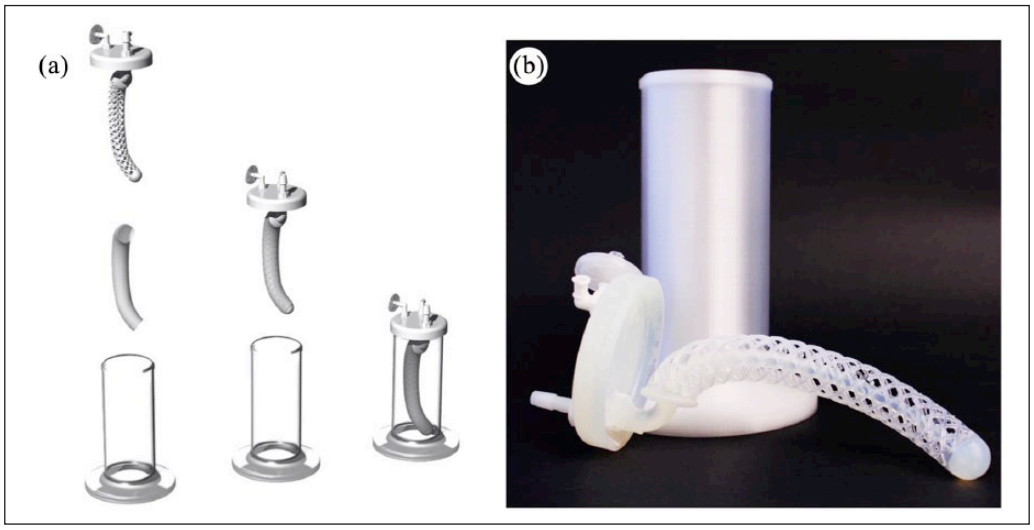

Figure 5. A custom patient-specific seeding apparatus was designed to accommodate the custom seeding mandrel. (a) Rendering of 3D-printed patient-specific closed-disposable seeding system. (b) Photograph of 3D-printed apparatus fabricated as a proof of concept.

Dark field imaging of seeded scaffold

A mid-graft sample of the seeded TEVG was embedded in O.C.T. Compound (Tissue-Tek, Sakura) and snap frozen on dry ice. Sections (10 µm thick) were prepared via microtome (Leica CM 1950) and mounted on positively charged slides (Superfrost™ Plus, Fisher Scientific). Slides were air-dried at room temperature for 30 min and then sections fixed with 10% neutral buffered formalin (Fisher Scientific) for 10 min. After two consecutive washes with 1× PBS 0.05% Tween-20 (5 min per wash), slides were stained with 4′,6-diamidino-2-phenylindole (DAPI, SlowFade™ Gold Antifade Reagent with DAPI, ThermoFisher Scientific) and coverslipped. Dark field photomicrographs were obtained with a Zeiss Axio Observer Z1 inverted microscope using an 89 North PhotoFluor LM-75 light source and the appropriate fluorescent filter at 20× magnification. Scaffold polymers were visualized by polarized light. Images were processed and merged using ImageJ (NIH).

CMR acquisition, reconstruction, and custom graft design

A CMR study was performed on a 1.5 T GE Signa Excite magnetic (General Electric Healthcare; Milwaukee, WI). Contrast-enhanced magnetic resonance angiography

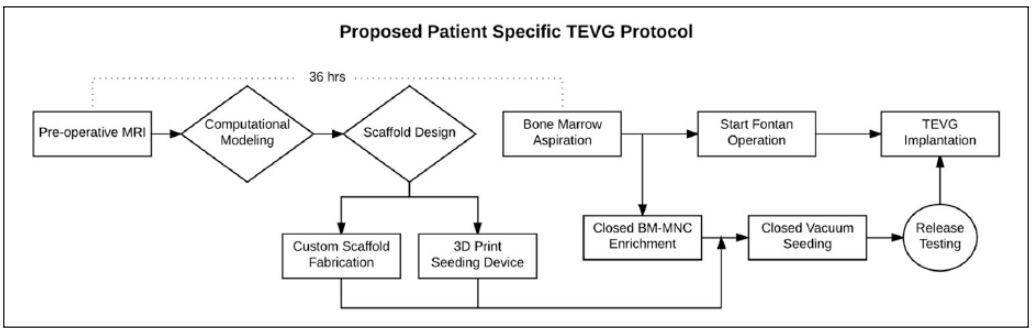

Figure 6. Incorporation of fluid dynamic and mechanobiologic computational modeling with additive manufacturing would permit a revised clinical protocol for design and preparation of the Fontan TEVG. Boxed items indicate process components, diamonds highlight a critical process decision, and circles indicate "go/no go" testing. Briefly, preoperative CMR would inform computational models to predict the optimal scaffold design. This design would be used to create a custom scaffold and 3D-printed seeding device. Bone marrow would be aspirated prior to start of the Fontan operation and a closed, disposable system for bone marrow mononuclear cell enrichment would be connected to the closed custom seeding apparatus. Vacuum seeding would be completed and samples collected for release testing prior to being implanted as a patient-specific Fontan conduit.

(MRA) of the chest was obtained after infusion of Gadofosveset trisodium (Ablavar® Lantheus Medical Imaging, Billerica, MA), an intravascular contrast agent to enhance both the cardiac and extra-cardiac structures. The acquired 3D dataset was then imported into a separate workstation for 3D processing using a specialized 3D rendering program (Vitrea Enterprise Suite Software 6.7.0, Vital, A Toshiba Medical Systems Company). After 3D reconstruction was performed by the Advance Processing Laboratory technician (A.T. and K.H.), the relevant anatomy including the inferior vena cava, pulmonary arteries, and pulmonary veins were identified. A custom-designed virtual graft was created that connected the inferior vena cava to the right pulmonary artery just proximal to the first upper lobe branch. The goal of the custom-designed virtual graft was to find the best pathway that avoided compression of the graft or other cardiac structures (pulmonary vein) as shown in Figure 3. This custom graft design was then used as a model for the CAD design and subsequent 3D-printing of the closed seeding apparatus.

CAD and 3D-printing

The cross-sectional area and centerline curve of the patient-specific conduit was imported into Rhino 3D for Mac (Seattle, WA). A scaffold wall thickness of 1 mm was assumed and a solid volume was created that represented the patient-specific TEVG. From this model a seeding mandrel was reverse-engineered with the following design features: >6 mm clearance between the scaffold and interior of the seeding chamber, a 3 × 20 mm thick base to stabilize the seeding chamber, a beveled cap creating an airtight seal once the scaffold and mandrel are in place, airtight Luer Lock fasteners for the BM-MNC input, 40 µm air filter, and suction tubing. After CAD modeling was complete, each individual component was exported in .stl format and opened in a .gcode slicing format (Cura 3.0.3 Geldermalsen, The Netherlands and Preform, Cambridge, MA). The seeding chamber was printed on an Ultimaker2 + Extended 3D printer (Geldermalsen, The Netherlands) with the following configuration: translucent PLA monofilament, 0.4-mm nozzle, 0.1-mm layer thickness 20% infill density, 90 mm/s print speed. The patient-specific mandrel and seeding cap was printed on a Form 2 3D printer (Cambridge, MA) with the following configuration: durable v1 resin, 0.1-mm print layer, support density of 1.00, and support point size of 0.70 mm. The seeding chamber and mandrel cap assembly were printed in parallel: the seeding chamber required 17 h to print and clean and the mandrel required 12 h.

Declaration of conflicting interests

The author(s) declared the following potential conflicts of interest with respect to the research, authorship, and/or publication of this article: C.Breuer is on the Scientific Advisory board of Cook Medical (Bloomington, IN), and C.Breuer and T.S. received research support from Gunze, Ltd (Kyoto, Japan) and Cook Regentec (Indianapolis, IN). Gunze, Ltd. kindly provided the scaffolds used in this study. C. Breuer and C. Best are cofounders of LYST Therapeutics, LLC (Columbus, OH). The remaining authors have no conflicts of interest to disclose.

Funding

The author(s) disclosed receipt of the following financial support for the research, authorship, and/or publication of this article: Research reported in this publication was supported in part by the National Heart, Lung, and Blood Institute of the National Institutes of Health under award number T32HL098039 (J.K.). The content is solely the responsibility of the authors and does not necessarily represent the official views of the National Institutes of Health.

References

1. Simeone RM, Oster ME, Cassell CH, et al. Pediatric inpatient hospital resource use for congenital heart defects. *Birth Defects Res A Clin Mol Teratol* 2014; 100: 934–943.

2. Benjamin EJ, Blaha MJ, Chiuve SE, et al. Heart disease and stroke statistics-2017 update: a report from the American Heart Association. *Circulation* 2017; 135: e146–e603.
3. Hoffman JIE and Kaplan S. The incidence of congenital heart disease. *J Am Coll Cardiol* 2002; 39: 1890–1900.
4. Rychik J, Goldberg D, Rand E, et al. End-organ consequences of the Fontan operation: liver fibrosis, protein-losing enteropathy and plastic bronchitis. *Cardiol Young* 2013; 23: 831–840.
5. Binns RL, Ku DN, Stewart MT, et al. Optimal graft diameter: effect of wall shear stress on vascular healing. *J Vasc Surg* 1989; 10: 326–337.
6. Trubel W, Moritz A, Schima H, et al. Compliance and formation of distal anastomotic intimal hyperplasia in Dacron mesh tube constricted veins used as arterial bypass grafts. *ASAIO J* 1994; 40: M273–M278.
7. Schmitz EJ, Kanar EA, Sauvage LR, et al. The influence of diameter disproportion and of length on the incidence of complications in autogenous venous grafts in the abdominal aorta. *Surgery* 1953; 33: 190–206.
8. Weston MW, Rhee K and Tarbell JM. Compliance and diameter mismatch affect the wall shear rate distribution near an end-to-end anastomosis. *J Biomech* 1996; 29: 187–198.
9. Thim T, Hagensen MK, Hørlyck A, et al. Oversized vein grafts develop advanced atherosclerosis in hypercholesterolemic minipigs. *BMC Cardiovasc Disord* 2012; 12: 24.
10. Ovroutski S, Ewert P, Alexi-Meskishvili V, et al. Comparison of somatic development and status of conduit after extracardiac Fontan operation in young and older children. *Eur J Cardiothorac Surg* 2004; 26: 1073–1079.
11. Downing TE, Allen KY, Goldberg DJ, et al. Surgical and catheter-based reinterventions are common in long-term survivors of the Fontan operation. *Circ Cardiovasc Interv* 2017; 10: e004924.
12. Hibino N, McGillicuddy E, Matsumura G, et al. Late-term results of tissue-engineered vascular grafts in humans. *J Thorac Cardiovasc Surg* 2010; 139: 431–436.e1–e2.
13. Patterson JT, Gilliland T, Maxfield MW, et al. Tissue-engineered vascular grafts for use in the treatment of congenital heart disease: from the bench to the clinic and back again. *Regen Med* 2012; 7: 409–419.
14. Drews JD, Miyachi H and Shinoka T. Tissue-engineered vascular grafts for congenital cardiac disease: clinical experience and current status. *Trends Cardiovasc Med* 2017; 27: 521–531.
15. Brennan MP, Dardik A, Hibino N, et al. Tissue-engineered vascular grafts demonstrate evidence of growth and development when implanted in a juvenile animal model. *Trans Meet Am Surg Assoc* 2008; 126: 20–27.
16. Toshiharu Shinoka GM. First report of histological evaluation of human tissue-engineered vasculature. *J Biotechnol Biomater* 2015; 5: 1–2.
17. Rocco KA, Maxfield MW, Best CA, et al. In vivo applications of electrospun tissue-engineered vascular grafts: a review. *Tissue Eng Part B Rev* 2014; 20: 628–640.
18. Freed LE, Vunjak-Novakovic G, Biron RJ, et al. Biodegradable polymer scaffolds for tissue engineering. *Biotechnology* 1994; 12: 689–693.
19. Marsden AL, Reddy VM, Shadden SC, et al. A new multiparameter approach to computational simulation for Fontan assessment and redesign. *Congenit Heart Dis* 2010; 5: 104–117.
20. Conover T, Hlavacek AM, Migliavacca F, et al. An interactive simulation tool for patient-specific clinical decision support in single-ventricle physiology. *J Thorac Cardiovasc Surg* 2018; 155: 712–721.
21. Ong CS, Loke Y-H, Opfermann J, et al. Virtual surgery for conduit reconstruction of the right ventricular outflow tract. *World J Pediatr Congenit Heart Surg* 2017; 8: 391–393.
22. de Zélicourt DA, Marsden A, Fogel MA, et al. Imaging and patient-specific simulations for the Fontan surgery: current methodologies and clinical applications. *Prog Pediatr Cardiol* 2010; 30: 31–44.
23. Yang W, Feinstein JA, Shadden SC, et al. Optimization of a Y-graft design for improved hepatic flow distribution in the Fontan circulation. *J Biomech Eng* 2013; 135: 011002.
24. Duan B. State-of-the-art review of 3D bioprinting for cardiovascular tissue engineering. *Ann Biomed Eng* 2017; 45: 195–209.
25. Hibino N. Three-dimensional printing. *World J Pediatr Congenit Heart Surg* 2016; 7: 351–352.
26. Anwar S, Singh GK, Varughese J, et al. 3D printing in complex congenital heart disease. *JACC: Cardiovasc Imag* 2017; 10: 953–956.
27. Fukunishi T, Best CA, Sugiura T, et al. Preclinical study of patient-specific cell-free nanofiber tissue-engineered vascular grafts using 3-dimensional printing in a sheep model. *J Thorac Cardiovasc Surg* 2017; 153: 924–932.
28. Fukunishi T, Best CA, Ong CS, et al. Role of bone marrow mononuclear cell seeding for nanofiber vascular grafts. *Tissue Eng Part A* 2018; 24: 135–144.
29. Mirensky TL, Hibino N, Sawh-Martinez RF, et al. Tissue-engineered vascular grafts: does cell seeding matter? *J Pediatr Surg* 2011; 45: 1299–1305.
30. Lee Y-U, Mahler N, Best CA, et al. Rational design of an improved tissue-engineered vascular graft: determining the optimal cell dose and incubation time. *Regen Med* 2016; 11: 159–167.
31. Roh JD, Sawh-Martinez R, Brennan MP, et al. Tissue-engineered vascular grafts transform into mature blood vessels via an inflammation-mediated process of vascular remodeling. *Proc Natl Acad Sci* 2010; 107: 4669–4674.
32. Best C, Tara S, Wiet M, et al. Deconstructing the tissue engineered vascular graft: evaluating scaffold pre-wetting, conditioned media incubation, and determining the optimal mononuclear cell source. *ACS Biomater Sci Eng* 2017; 3(9): 1972–1979.
33. Kurobe H, Maxfield MW, Naito Y, et al. Comparison of a closed system to a standard open technique for preparing tissue-engineered vascular grafts. *Tissue Eng Part C Methods* 2015; 21: 88–93.
34. Kurobe H, Tara S, Maxfield MW, et al. Comparison of the biological equivalence of two methods for isolating bone marrow mononuclear cells for fabricating tissue-engineered vascular grafts. *Tissue Eng Part C Methods* 2015; 21: 597–604.
35. Hibino N, Nalbandian A, Devine L, et al. Comparison of human bone marrow mononuclear cell isolation

methods for creating tissue-engineered vascular grafts: novel filter system versus traditional density centrifugation method. *Tissue Eng Part C Methods* 2011; 17: 993–998.
36. Elomaa L and Yang YP. Additive manufacturing of vascular grafts and vascularized tissue constructs. *Tissue Eng Part B Rev* 2017; 23: 436–450.
37. Pedde RD, Mirani B, Navaei A, et al. Emerging biofabrication strategies for engineering complex tissue constructs. *Adv Mater* 2017; 29: 1606061.
38. Sears NA, Seshadri DR, Dhavalikar PS, et al. A review of three-dimensional printing in tissue engineering. *Tissue Eng Part B Rev* 2016; 22: 298–310.
39. Udelsman B, Hibino N, Villalona GA, et al. Development of an operator-independent method for seeding tissue-engineered vascular grafts. *Tissue Eng Part C Methods* 2011; 17: 731–736.
40. Miller KS, Lee YU, Naito Y, et al. Computational model of the in vivo development of a tissue engineered vein from an implanted polymeric construct. *J Biomech* 2014; 47: 2080–2087.